Acta Psychologica 37, 375–392. © North-Holland Publishing Company 1973

DEPTH OF VISUAL INFORMATION PROCESSING*

Irwin POLLACK
University of Michigan, Ann Arbor, U.S.A.

The depth of visual information processing is identified with the longest randomly-generated binary-encoded spatial pattern whose partial repetitions can be detected. In contrast with the auditory detection of sequentially-presented constraints, the depth of perceptible visual encoding of spatially-presented constraints is sharply limited. Depths of about 35 were achieved for one-dimensional constraints; depths of perhaps 3 or 4 were achieved for two-dimensional constraints imposed in only one direction and depths of perhaps 2 for two-dimensional constraints imposed in two directions. With one-dimensional constraints, it is shown that the inferred depth of processing is partially determined by the number of pattern representations and by the spatial distance between successive representation for visual displays of fixed size.

1. Introduction

Julesz (1962) has suggested an operational measure for defining the depth of visual information processing: depth of processing is identified with the largest random signal whose partial periodicities can be detected. In determining the depth of temporal processing, for example, one seeks to determine the longest random sequence for which observers can identify repetitions of the random sequence from independently determined random sequences. Discrimination breaks down for auditory random noise sequences of 1–4 sec (Guttman and Julesz 1963; Julesz and Guttman 1963). Comparable experiments have not been reported in vision, but preliminary research indicates a comparable duration of 250–500 msec for two-dimensional random-dot visual patterns.

* This research was supported in part by Grant GB 14036X of the National Sciences Foundation. The writer is indebted to Mrs. Nancy Mandell for supervising the experimental tests; to Lon Radin for the PDP-8I computer program; to Don Mayer for an extension of the 8I program to the extended display format and to distributed patterns; to Louis Wojnaroski for the PDP-9 computer program; to Robert Shea for processing the experimental results; and to Kenneth Bachman for developing high-speed plotting hardware for the PDP-9.

The depth of spatial processing may be similarly defined. Here one seeks to determine the largest random visual pattern for which observers can identify repetitions of the random visual patterns from independently determined patterns. With partial repetition – rather than exact repetition – Julesz (1962) showed that the discernible depth for spatially-encoded displays in one dimension was only 3 or 4 elements of the random sequence. Specifically, Julesz employed a procedure developed by Rosenblatt and Slepian (1962) which controls the probability of a parity sum over n successive elements. In this method, constraints are absent within n successive elements; constraints are imposed between elements n units removed from each other. The Rosenblatt–Slepian procedure, however, required encoding of display elements into more than two states for higher-order sequences, and Julesz employed several levels of brightness for encoding. Perhaps the estimate of the depth of spatial processing was restricted by the requirement of multilevel brightness encoding. Might we achieve higher discriminable depths with binary-coded displays?

A related procedure of distributing statistical constraints, which is applicable to binary-coded elements, was developed by Smith (1954). A set of n sub-sequences, each k units long, is developed, each with the same sequential repetition probability. The independently-derived n sequences are then interfolded into each other. The first n elements of the merged sequence consist of the first element of each of the n sub-sequences; the second n elements of the merged sequence consist of the second element of each of the n sub-sequences,... the k-th n elements of the merged sequence consist of the k-th element of each of the n sub-sequences. As in the Julesz procedure, the discernible depth of processing, n, can be identified. Tests in audition (Pollack 1969) show that the upper limit upon n is reached by the capability of discrete sequence generators before the ear's limit can be discerned.

The present tests explore the upper limit on the descernible depth of spatial enfolding for visual displays. In particular, we shall identify the depth of information processing with the largest randomly-generated pattern for which pattern-repetitions can be detected.

2. Method

2.1. Preliminary informal tests

Random dot patterns consisting of dots and non-dots were drawn upon 28 X 34 cm paper sheets by a computer printer. The probability of a dot at each position of an imaginary 50 X 80 grid was 0.5; the column density was 2.5 position/cm and the row density was 4 positions/cm.

Observers viewed a large display consisting of 16 separate sheets, arranged in two rows of 8 patterns each. One row consisted of the same random pattern on 8 adjacent sheets; one row consisted of 8 independent patterns on 8 adjacent sheets. The subject's task was to respond which one of the two rows employed the repeated pattern. The patterns were initially viewed from a distance of 10 meters. The subject was instructed to walk toward the display until he could identify the row of repeated patterns.

Typical behavior was to approach the displays closely until some unusual local feature was identified upon a single sheet and then to test whether that feature was found on adjacent sheets. That is, the problem was solved by deliberate analysis; the periodicities did not stand out in immediate experience. The data do indicate, however, that with slow, deliberate analysis, exact repetitions of a large random pattern can be perceived. Therefore in the main tests, partial periodicities were introduced to random patterns. Thresholds were defined in terms of the degree of repetition required for a fixed level of performance.

2.2. One-dimensional constraints

2.2.1. Generation of sequences

One-dimensional Markov spatial constraints were generated by controlling the conditional repetition probability of binary-encoded sequences, $P(A|A)$. Such sequences, when converted to displays of dots and no dots, yield long unbroken sequences of dots and of no dots at high $P(A|A)$ levels, as seen in the upper left corner of fig. 1, and yield rapidly alternating sequences of dots and no dots at low $P(A|A)$ levels. The average run length of identical elements within such sequences is $1/[1 - P(A|A)]$.

Consider a folded Markov sequence, initialized by an unconstrained random sequence of W elements, and laid down as the first row of a display of width W. Each element of the initial random sequence becomes the initial element of a constrained sequence, to be determined by $P(A|A)$ in successive columns. For example, if the initial element was a dot, at high $P(A|A)$ levels, a sequence of dots would tend to be generated; if the initial element was a space, at low $P(A|A)$ levels, a sequence of spaces and dots, starting with a space, would tend to be generated. If each element of the initial random sequence heads one column of the display, the several constrained sequences would appear as vertical columns of the display.

The method is illustrated for a 4 X 4 matrix in the first line of table 1 for $D = 1$. An initial unconstrained binary-coded random sequence is laid down in positions *a, b, c, d.* Each binary element in positions *a, b, c* and *d* becomes the starting element of a sequence which is continued by $P(A|A)$. The first constrained sequence is laid down in positions *a, e, i, m*; ... the fourth sequence is laid down in positions *d, h, l, p.*

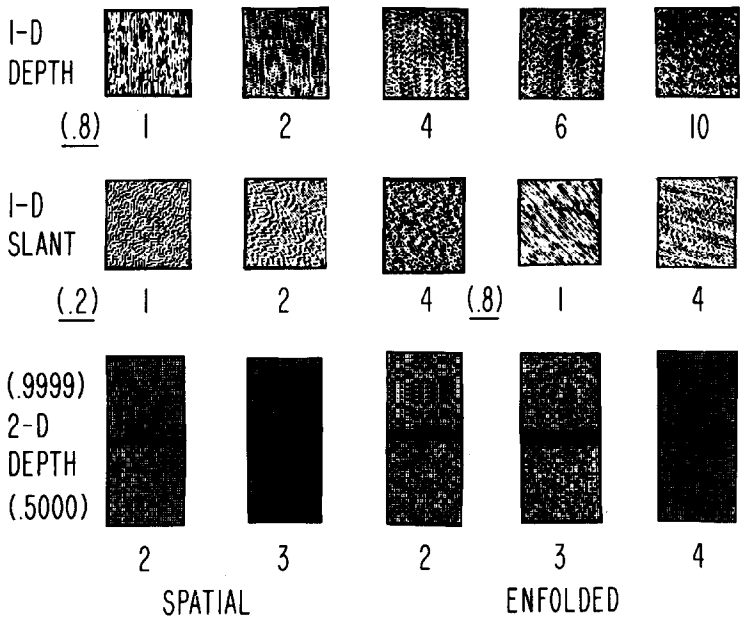

Fig. 1. Examples of one-dimensional and two-dimensional enfolded Markov constraints. Under each display is the depth of folding (top and bottom lines) or the slant (middle lines). The associated $P(A|A)$ or $P(S_e)$ level is shown in parentheses to the left of the displays. Displays with 1–D constraints were developed in a 60 × 60 matrix; displays with 2–D constraints were developed on a pair of 32 × 32 matrices, the top matrix was set at $P(S_e) = 0.9999$ and the bottom at $P(S_e) = 0.5$. Differences in photographic density and size were not present in original displays.

Table 1
Illustration of derivation of folded Markov sequences.

Matrix positions	D	s	Initial random	Examples of sub-sequences
a b c d	1	0	*a–d*	*a e i m, d h l p*
e f g h	2	0	*a–h*	*a i, d l, e m, h p*
i j k l	1	1	*a–e*	*a f k p, e j o–d*
m n o p	2	5	*a–i*	*a j, e n, d–i, h–m*

2.2.2. Depth

Consider now a folded Markov sequence, initialized by an unconstrained random sequence of DW elements, where D is an integer, n, and laid down as the first D rows of the display of width W. Again, each initial element is associated with an independently generated sequence. Successive elements within the same sequence are derived according to $P(A|A)$, but are spatially separated by $(D-1)$ independently derived elements. For example, when $D = 2W$, within any given column, elements in the odd rows represent one generating sequence; elements in the even rows represent another; and, elements in the odd rows are independently derived from elements in the even rows. The method is illustrated for a 4 × 4 matrix in the second line of table 1 for $D = 2$. The initial unconstrained random sequence is laid down in positions a through h. Each of these positions heads up a constrained sequence, e.g. *ai,...dl*, *em...hp*. The variable D will refer to the depth of encoding of one-dimensional constraints. Examples of various depths of encoding of one-dimensional constraints upon a 60 × 60 element display are given in the top line of fig. 1 for $P(A|A) = 0.80$.

In anticipation of the results, it should be noted that there are several effects of varying D. First, since the number of constrained elements is the width of the display (W) times the length (L) minus the initial randomizing sequence, the total number of constrained elements is $(L-D)W$. Variation in D is inconsequential for $D<<L$. More important is that the number of display elements within each constrained sequence, including the initializing element, is L/D; and the total number of independently generated sequences contributing to the constraints is DW.

2.2.3. Introduction of noise

Noise was introduced in the form of unconstrained random *sequences*, $P(A|A) = 0.5$, into the displays. Had random elements, rather than random sequences, been introduced, the targetted $P(A|A)$ levels would simply have been modified. The introduction of 50% random elements into a display with $P(A|A) = 0.70$, for example, leads to a display with $P(A|A) = 0.5(0.7) + 0.5(0.5) = 0.60$. The introduction of 50% random columns into a display permits O to filter the constrained from the unconstrained sequences. In table 1, such a display might consist of random sequences at positions $a-m$ and $d-p$, and, constrained sequences at positions $b-n$ and $c-o$.

The positions of the unconstrained sequences were randomly chosen. Unconstrained sequences, therefore, have several effects: they displace constrained sequences from the display; they break up adjacent clumps of constrained sequences, and they hide or mask the presence of constrained sequences.

2.2.4. Slant

We now turn to a related variable, slant, s. Consider a folded Markov sequence, initialized by an unconstrained random sequence of $(W+s)$ elements, where s is a small integer when compared to W. The sequence is laid down in a display of width W. Each initial element is again associated with an independently generated sequence by means of $P(A|A)$. Elements of the same sequence are plotted in different columns. For example, an initial random sequence of 61 units is laid down in the top row of a display of 60 columns, with the 61st element laid down in the first column of the second row. The second random sequence of 61 elements is laid down in the remaining 59 columns of the second row with the 60th and 61st elements laid down in the first two columns of the second row... In this way, one sequence is laid down upon the diagonal elements of a square matrix, and other sequences are laid down parallel to the diagonal element. In general, the slant s, $= \Delta W/\Delta L$. The method is illustrated for a 4 × 4 matrix in the third line of

table 1 for $D = 1$, $s = 1$, i.e., with the initial sequence a–e of 5 units with a display of width 4. Only the diagonal sequence is unbroken; all other sequences are broken, e.g., *e, j, o* and *d*.

Slant may also be combined with depth by employing initializing sequences of length $D(w+s)$. The method is illustrated for a 4 × 4 matrix in the fourth line of table 1 for $D = 2$, $s = 0.5$. Examples of various slant levels for the 60 × 60 display are given in the second line of fig. 1. The first three displays represent $P(A|A) = 0.20$; the last two represent $P(A|A) = 0.80$.

In anticipation of the results, it is noted that the effects of slant are different from simply turning vertically generated constraints to the appropriate slant angle. Even without the depth variable added to the slant variable, the effects of slant parallel those of depth. For a slant of 1, for example, only the diagonal sequence is of length W, when $W = L$, and off-diagonal sequences become shorter and shorter so that the average length of slanted sequences is $W/2$. In general, the average length of slanted sequences is $W/(1+s)$.

2.2.5. Procedure

Displays were painted on the face of a Tektronix 601 display equipped with a P4 storage tube. Natural binocular viewing was employed. The distance to the display was controlled by *O* for maximal comfort, but averaged about 50 cm. The inter-dot separation was 0.77 mm between successive columns and 0.83 mm between successive rows. Four 60 × 60 matrices were presented in a 2 × 2 array. Three of the four matrices obeyed a reference constraint level, $P(A|A)_R$; one obeyed a variable constraint, $P(A|A)_V$. The position of the odd display was randomly varied. The task of *O* was to indicate the position of the odd matrix. An adaptive stimulus programming procedure (Taylor and Creelman 1967) varied $P(A|A)_V$ to converge upon 50% correct in the four-alternative, forced choice (4AFC) test. The duration of the display was determined by *O*. He was encouraged to respond quickly by means of instructions and by an incentive schedule based upon the number of completed thresholds. A PDP-8I computer generated the displays and executed the adaptive programming procedure (details in Pollack 1972).

In order to achieve a larger number of pattern repetitions, additional tests were carried out with 15 × 240 matrix displays arranged in a 1 × 4 array. Otherwise, details were identical.

When the adaptive procedure sought $P(A|A)$ levels below 0 and above 1.0, one trial was provided at the extreme condition. An incorrect response at the extreme condition terminated the trial. The proportion of terminated trials, $P(T)$, thus, provides a rough measure of extreme difficulty. For conditions with $P(T) \leqslant 0.10$, thresholds are represented by geometric means, excluding the terminated trials; for conditions with $P(T) > 0.10$, thresholds are represented by medians, including terminated trials. Half-filled points represent conditions with $0.10 < P(T) \leqslant 0.20$. Filled points represent conditions with $P(T) > 0.20$. The degree of shading of the points, then, represents a crude display of discriminability.

2.3. Two-dimensional constraints

2.3.1. Generation of sequences

Two-dimensional Markov spatial constraints were generated by controlling a parity sum among overlapping 2 × 2 cells of the matrix. In the context of a binary code where, for example, a dot is represented by 1 and a space is represented by 0, an even parity sum consists of 0, 2 or 4 dots within a 2 × 2 local unit; an odd parity sum consists of 1 or 3 dots.

Specifically, the first row and the first column of a 32 × 32 matrix were determined by unrestricted random sampling (except for the overlapping intersecting element). In the local 2 × 2 matrix of the upper left corner, three of the four elements are defined. The fourth is determined by the parity sum. After the initial fourth element is determined, the next 2 × 2 matrix has three entries given and the fourth element is determined by the next parity sum.

Variation in the probability of an aimed-for even parity sum, $P(S_e)$, controls the organization of the display. At high $P(S_e)$ levels, rectangular clumps of dots and non-dots are obtained in checkerboard patterns; at low $P(S_e)$ levels, distributed or "lacey" displays are obtained.

The procedure just described can be extended to different depths of enfolding. Consider two submatrices, each with 16 rows and 32 columns. Two-dimensional constraints are developed for each submatrix and then the rows are interfolded. Thus, items on odd rows of the merged 32 × 32 matrix were developed from one 16 × 32 submatrix; items on even rows were developed from the other submatrix. In general, a depth of enfolding by rows alone, D, is achieved by developing D submatrices, subjecting each to $P(S_e)$, and then interfolding by rows. The right three displays on the lowest line of fig. 1 illustrate the effect of D with row enfolding. Each figure represents a pair of 32 × 32 matrices, the upper one at $P(S_e) = 0.9999$; the lower one at $P(S_e) = 0.50$. Discrimination is barely possible with $D = 3$ or 4.

The enfolding procedure may be further extended to obtain two-directional, or spatial, enfolding. Consider the case of $D = 2$. Four 16 × 16 submatrices develop two-dimensional constraints by $P(S_e)$. Matrices 1 and 2 are enfolded by rows, as are matrices 3 and 4, to form two intermediate 16 × 32 matrices. These intermediate matrices are then enfolded in terms of alternative columns to make a 32 × 32 matrix with $D = 2$ in both directions. In general, n^2 submatrices are first developed; n intermediate submatrices are formed by row enfolding; the remaining n intermediate matrices are then enfolded by columns. The left two displays on the lowest line of fig. 1 illustrate two-dimensional enfolding. Discrimination is barely possible with $D = 3$.

2.3.2. Procedure

Displays were painted on the face of a Tektronix 602 display equipped with a fast P-15 phosphor. A PDP-9 computer generated the displays and executed the adaptive programming procedure. Details were otherwise identical with the one-dimensional tests, except that $P(S_e)_R$ replaced $P(A|A)_R$ and $P(S_e)_V$ replaces $P(A|A)_V$. The inter-dot spacing was 1.17 mm and the average seating distance was 70 cm. Over the one- and the two-dimensional tests, 230 experimental conditions were employed with each of at least 15 observers contributing two thresholds, for a total of 6.9×10^3 thresholds.

3. Results

3.1. One-dimensional constraints

3.1.1. Measure

Thresholds will be expressed in terms of the average conditional repetition probability of one of the two states, $P(\cdot|\cdot)_V$, required for 50% correct response in the 4AFC test. It is noted that the conditional repetition probability of the non-dot state equalled that of the dot state.

3.1.2. Constant display size

Fig. 2 explores the role of pattern depth for one-dimensional constraints for a 60 × 60 display of 3600 elements. For this display, the product of depth, D and the number of repetitions of the pattern, R, is constant at 60. Increment thresholds above the indicated reference conditional repetition levels (parameter) are plotted in the left section; decrement

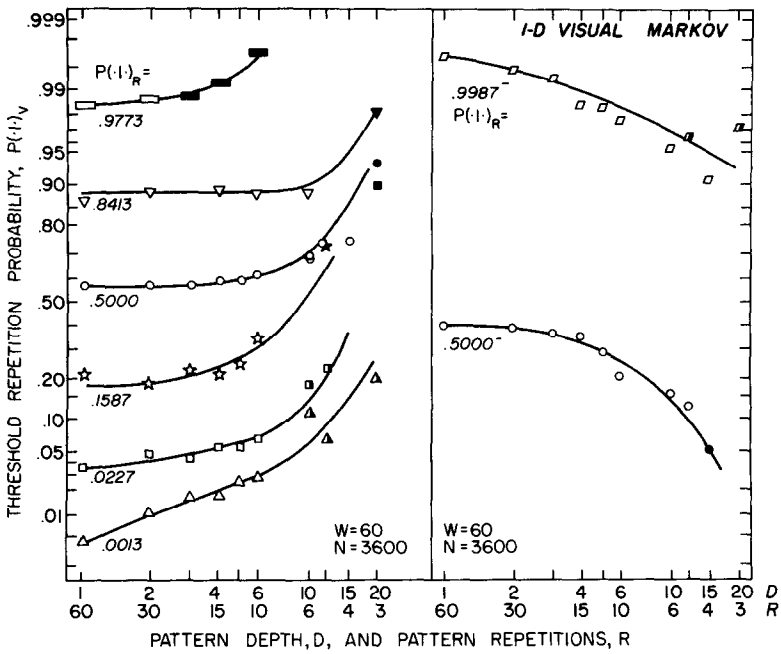

Fig. 2. Effect of pattern depth, D, and the number of pattern repetitions, R, for threshold increments (left section) and decrements (right section) as a function of the reference $P(A|A)$ level (parameter). Displays with a constant number of elements.

thresholds below the indicated reference levels are plotted in the right section. The ordinate scale is that of the standard-score transform of the normal probability curve.

Since the successive reference levels represent equal differences in standard scores in the left section, the nearly equal spacing of the threshold curves suggests that nearly a constant standard-score difference separates the threshold and reference levels, at least for low depths of enfolding. Performance suffers, i.e. threshold differences increase in magnitude, at longer depths of enfolding (and/or at a smaller number of pattern repetitions). Under selected conditions, a depth of 15 can be discriminated with displays of length 60.

3.1.3. *Interaction of pattern depth and number of pattern repetitions*

The complete confounding between pattern depth, D, and pattern repetitions, R, in the tests of fig. 2 is removed in the tests of fig. 3. Depth, as represented by the symbols, and pattern repetitions, as represented by the abscissa, were independently varied. The three sections represent displays of 1, 6 and 60 columns in width. Thresholds are jointly determined by D, the pattern depth; by R, the number of pattern repetitions; and by W, the width of the pattern. No simple tradeoff is noted, but consistent discrimination is observable with $D = 15$. With only 60 rows, however, it is not clear if the apparent upper depth limit is determined more heavily by the number of pattern repetitions, a maximum of 4 with $D = 15$, or by the depth of the sequence.

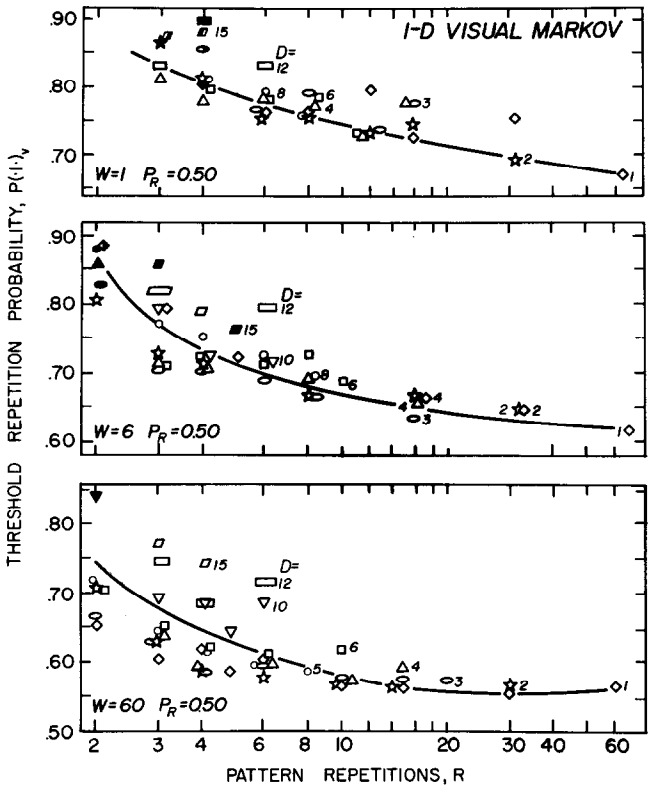

Fig. 3. Effect of pattern depth (parameter) and number of pattern repetitions (abscissa) for display-widths of 1 (top section), 6 (middle section) and 60 (bottom section) display elements. The length of the display is the product of pattern depth and the number of pattern repetition.

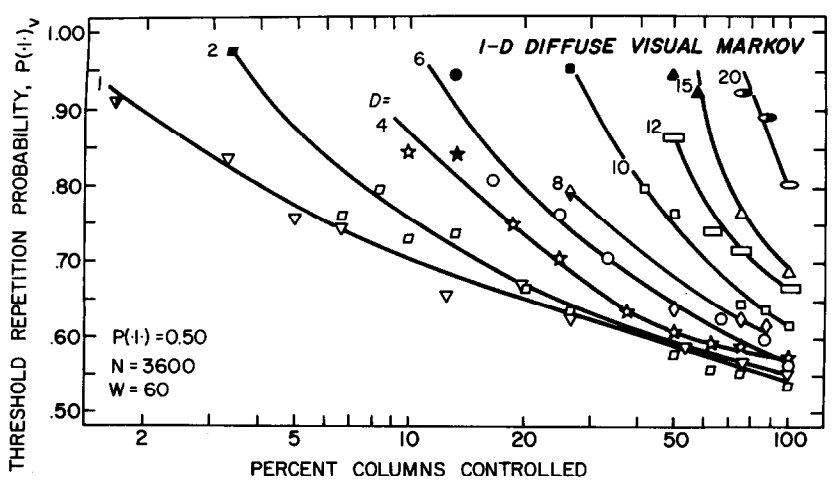

Fig. 4. Effect of unconstrained random sequences ('noise') on the detection of partial periodicities as a function of pattern depth (parameter) and the fraction of sequences controlled (abscissa). The percentage of unconstrained sequences was 100 minus the percentage of controlled columns.

3.1.4. Effect of noise

The effect of introducing noise into patterns of different depth is examined in fig. 4. Patterns of low depth are relatively resistant to noise – a single sequence at a high $P(A|A)$ level at $D = 1$ can be detected. Longer depths require a greater proportion of controlled sequences for pattern detection.

3.1.5. Effect of slant

Fig. 5 examines the effect of slant, s. The lower section considers one-dimensional increment constraint thresholds above a chance reference constraint as a function of slant and of depth (abscissa), relative to a chance reference constraint. For a depth of 1, thresholds rise sharply only at the higher slant levels. Sharp changes occur at lower and lower slant levels at higher and higher depths of encoding. This result suggests that the interaction of depth and slant may have a common basis with respect to the deterioration of discrimination. However,

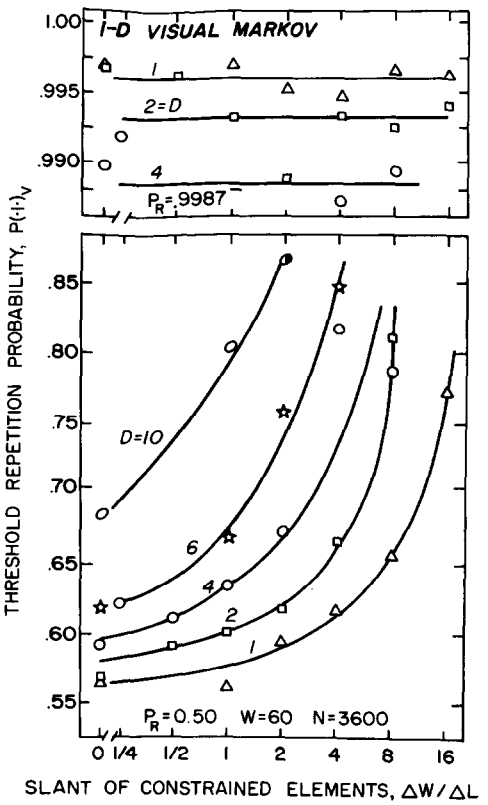

Fig. 5. Combined effect of pattern slant (abscissa) and pattern depth (parameter) upon detection thresholds for increments above a chance reference level (lower section) and decrements below a near-perfect reference level (upper section).

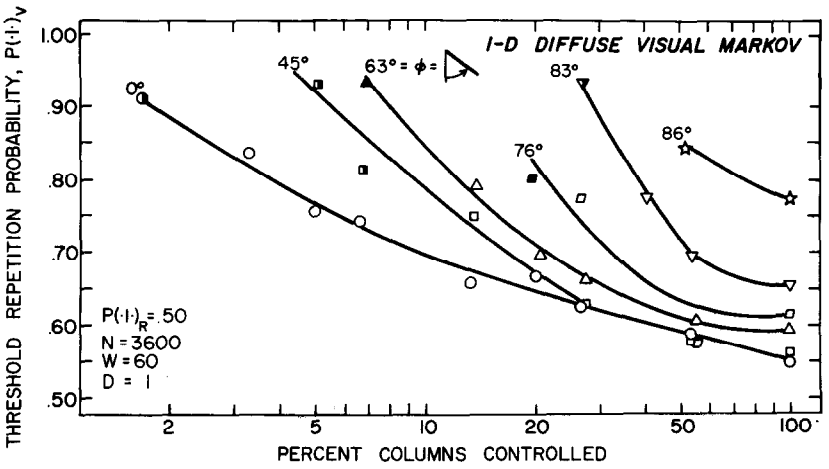

Fig. 6. Effect of unconstrained random sequences ('noise') on the detection of partial periodicities as a function of the slant angle from the horizontal (parameter) and the fraction of sequences controlled (abscissa).

the top section, which represents decrement thresholds below a near-perfect constraint level shows little additive effect of slant and depth.

The effect of introducing noise into patterns of different slant is examined in fig. 6. (Slant is expressed in terms of the direction of constraint relative to a horizontal line; $s = 0$ is represented at 90°.) As with pattern depth, higher degrees of slant can be detected only with a high proportion of controlled columns.

3.2. Two-dimensional constraints

3.2.1. Measure

Thresholds will be expressed in terms of the probability of an even parity sum, $P(S_e)_V$, required for 50% correct response in the 4AFC test.

3.2.2. Depth

Fig. 7 considers the effect of the depth of enfolding (in one direction) for the detection of two-dimensional constraints. The left section represents increment thresholds above a chance reference constraint level; the right section represents decrement thresholds below a perfect constraint level. The parameter is the depth of encoding; the abscissa is the display duration, expressed in terms of the number of display paintings, each 18 msec in duration. The single point in parentheses in the left section represents a decrement threshold of 0.09 relative to a reference constraint of 0.50, but plotted in terms of its reflection above 0.50 on the ordinate.

Discrimination improves as a function of display duration. Increment thresholds (left section) are obtainable for $D = 3$, and perhaps $D = 4$, for extremely long display exposures (nearly 10 sec). Decrement thresholds (right section) are obtainable for $D = 3$, and perhaps $D = 4$, for extremely long display exposures.

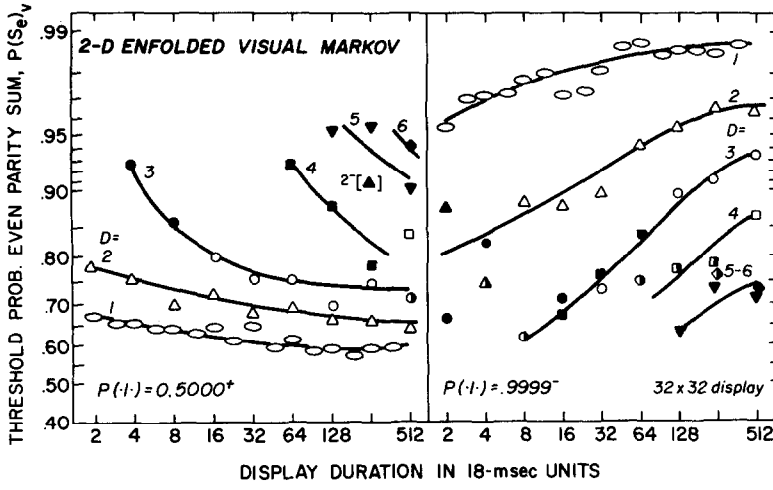

Fig. 7. Increment (left section) and decrement (right section) thresholds for two-dimensional constraints as a function of the depth of enfolding (parameter) and display duration (abscissa). The point within brackets represents a decrement threshold at 0.09, relative to the chance reference level of 0.50.

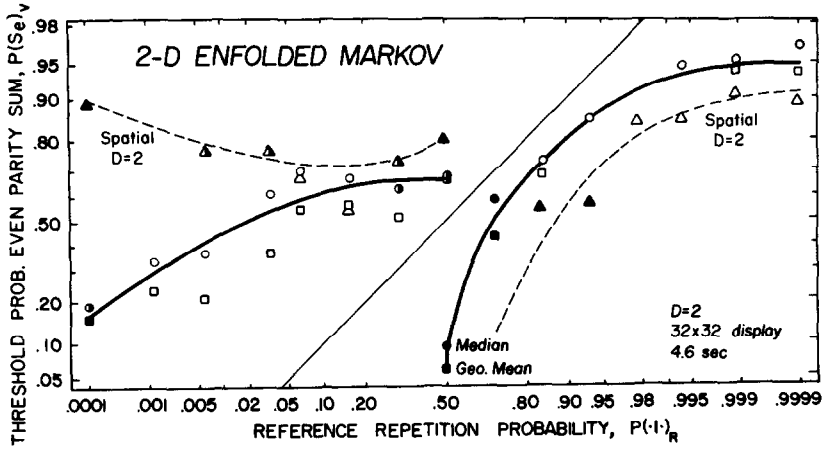

Fig. 8. Increment (above chance reference line) and decrement (below chance reference line) thresholds for two-dimensional enfolded constraints. The dashed curve and triangles represent spatial enfolding (in two dimensions). The coordinates are the normal probability grid.

3.2.3. One-directional spatial enfolding

Fig. 8 compares increment thresholds (above the diagonal reference line) and decrement thresholds (below the diagonal reference line) for one-directional and for two-directional enfolding of $D = 2$. Both medians (circles) and geometric means (squares) are presented for one-directional enfolding. The coordinates are normalized in each direction. Sharp differences from the reference line are observed. Upon such coordinates, two-dimensional constraint thresholds, with $D = 1$, plot as nearly straight lines parallel to the reference line (Pollack 1972). With $D = 2$, there is a marked departure from such functions.

3.2.4. Two-directional enfolding

Two-directional spatial enfolding (triangles) requires substantially larger threshold deviations than one-directional enfolding. Under selected conditions, consistent thresholds can be achieved for spatial enfolding $D = 2$ only for a limited range of conditions. Comparison between common conditions of figs. 7 and 8 suggests that two-dimensional constraint thresholds obtained with two-directional spatial enfolding, with $D = 2$, are nearly equivalent to those obtained with one-directional enfolding with $D = 3$ or 4.

4. Discussion

4.1. Comparison with Julesz' estimate of the depth of processing

In the Rosenblatt–Slepian procedure employed by Julesz, the number of states of the sequence must increase with the depth of constraint. The apparent mismatch between Julesz' estimate of depth of processing at 3–4 and the present estimate of depth of 15–20 is probably related to the present use of binary coded sequences at all depths.

4.2. Auditory temporal vs visual spatial depths of processing

The limit on the temporal depth of auditory processing is a temporal limit. When expressed in terms of the number of samples required for a bandwidth of 20 kc, a 4-sec limit translates to 160,000 numbers which must be specified to determine the random noise waveform. There, sample i is correlated with sample $(160{,}000 + i)$, but all numbers within each block of 160,000 are independent. No direct comparison can be made with spatial depths of visual processing, because visual displays can be generated in two dimensions. Thus, folded Markov sequences can be generated with contingencies separated by DW elements. When such a sequence is laid down upon a display of W elements in width, contingencies are separated by depth D, as in the present tests. Defini-

tion in terms of the initial *DW* separation might yield estimates close to the 160,000 of the auditory sequence. Such an estimate, however, is misleading because displays of arbitrary width can be generated.

4.3. Display limitation

The display for one-dimensional constraints was limited to 60 X 60 matrices and the apparent upper depth limit was 15 or four pattern replications. If a minimum of four pattern replications is required, the upper depth level may be more nearly display-limited, rather than operator-limited.

Fig. 9 presents the results of tests with the 15 X 240 display which provided a greater number of pattern replications for displays of a given depth. The parameter is the depth of the pattern. The proportion of terminated trials is roughly indicated by markings: no marking (0–10%), tic mark (10–20%), a single underlying bar (20–50%), and a double underlying bar (>50% terminated trials). Two curves are drawn: the dashed curve showing thresholds with 3600 elements; and, the solid curve representing the lower limit with $D = 1$. Discrimination is possible for depths between 30 and 40 with 5–6 pattern replications.

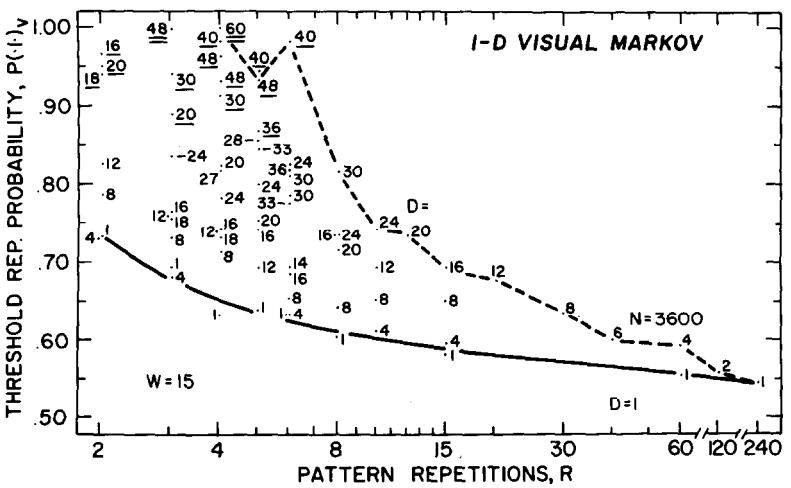

Fig. 9. Effect of pattern depth (parameter) and number of pattern repetitions (abscissa) on the detection of one-dimensional constraints for a 15 X 240 display configuration. The proportion of terminated trials is indicated by the bar code (see text). The two curves represent: performance with 3600 display elements; and performance with $D = 1$.

4.4. Alternative views of the pattern depth variable

Why does performance break down at large D levels? Perhaps the number of display elements in the entire pattern, DW, is crucial. This alternative would predict that the discriminable depth, D, would increase as the width of the display, W, is decreased. However, fig. 3 shows that the opposite result obtains. We must, therefore, look to other alternatives.

Pattern depth in one-dimensional displays has several consequences. For displays of fixed size, the smaller pattern depth, the larger the number of pattern repetitions. Figs. 3 and 9 showed, however, that for a fixed number of pattern repetitions, lower thresholds are obtained with smaller pattern depths. The exception concerns 2–3 repetitions with narrow displays, where shorter pattern lengths provide an insufficient number of display elements.

Two additional factors favor shorter pattern depths: the starting positions of successive representations of a longer pattern may be more difficult to recognize than for a shorter pattern; and, corresponding positions within longer patterns are separated by larger distances than within shorter patterns. Each of these features may be examined experimentally.

The 15 X 240 display was employed with 6 pattern representations, but each representation was separated by 2 rows (1.8 mm additional space) upon the display. In this way, each representation of the pattern was marked for O. The thresholds from such tests are presented as squares and the broken line in the left section of fig. 10; corresponding thresholds obtained in the original tests without demarcation are shown as circles and the non-broken line. There is a consistent difference in favor of the unbroken display. This result was unexpected but may be related to the O's remarks that the broken display imposes order upon the random replications. We may tentatively conclude that the primary advantage of the shorter patterns does not stem from the better identification of their starting positions.

The 15 X 240 display was employed so that the first lines of successive pattern representations were separated by constant distances, irrespective of the length of the pattern. This was accomplished by introducing blank rows between pattern representations. Six pattern representations again were employed. The results are presented in the right section of fig. 10. The parameter on the curves is the distance, in rows,

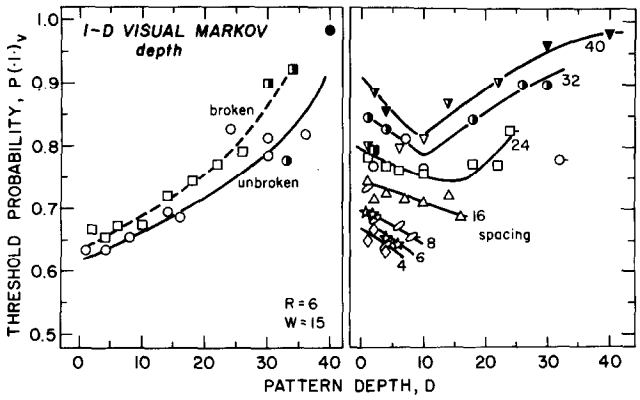

Fig. 10. Effect of pattern demarcation and spacing on the detection of partial periodicities as a function of pattern depth (abscissa). The left section contrasts non-broken (circles) patterns and demarcated (squares) patterns separated by 2 display rows. The parameter of the right section is the spacing, in terms of the number of display rows, between corresponding elements. The spacing between successive rows was 0.83 mm. The tic marks identify non-marked patterns where the spacing equalled the pattern depth.

between corresponding lines of successive pattern representations. When the spacing distance equalled the pattern length, no demarcation was provided, and the corresponding thresholds are plotted with tic marks.

The major result is that thresholds *decrease* up to intermediate pattern lengths, for a fixed spacing. Stated otherwise, partial periodicities are easily detected within short patterns because statistically related elements are closely spaced, not simply because less processing is required for shorter than for intermediate pattern lengths. Even with a fixed spacing, however, discrimination suffers with longer patterns. Although the observer could simply ignore segments of the longer broken patterns, he apparently was unable to do this. The apparent limit on the visual processing of partial spatial periodicities is, therefore, determined by spatial, as well as by informational, factors.

4.5. Displays of controlled duration

In the previous one-dimensional tests, the duration of the display was uncontrolled. Are the conclusions reached in the previous section limited to displays of unlimited duration? Additional tests were carried out

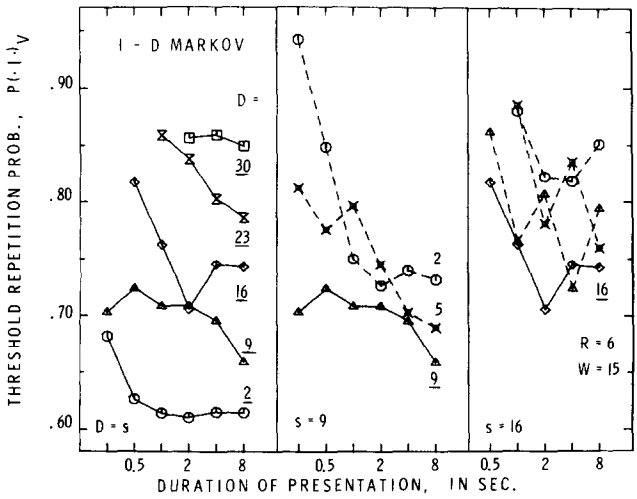

Fig. 11. Effect of duration (abscissa) on one-dimensional constraint thresholds (ordinate) for different pattern depths (parameter). The left panel represents non-separated patterns where spacing = depth. The middle and right panels represent increasing degrees of spacing between corresponding elements of a pattern. The solid lines connect conditions with non-separated patterns. The dashed curves reflect conditions with separated patterns.

over 117 experimental conditions with the 15 X 240 display. The display storage persisted for 0.25 to 8 sec following the initial painting of the display. The other independent variable was the depth of patterning. (The initial painting time for each of the four displays was 5.2 times D msec.)

The left panel of fig. 11 considers displays without additional separation. The abscissa of all panels is the additional duration of the display; the ordinate is the threshold level; the parameter is the depth of patterning. Over the range from 0.5 to 8 sec, thresholds appear to change more for patterns of greater depth than for patterns of a lower depth. The apparent exception is for the largest depth levels, where a substantial portion of the trials was terminated, and a ceiling effect is obtained.

The middle and right panels reflect thresholds for fixed spacings of 9 and 16 elements, consisting of non-separated displays (solid lines and underlined parameters) and separated displays (dashed lines and non-underlined parameters). Additional tests were also run with spacings of 23 and of 30 elements. Their results confirm the trends shown with spacings of 9 and 16 elements. As the spacing among elements is in-

creased, thresholds increase. For a fixed spacing, within each panel, no consistent penalty is suffered at the larger pattern depths. Indeed, highest thresholds are obtained for the smallest pattern when separated. The overall conclusion from fig. 11 is that separation is the controlling variable over a wide range of exposure durations.

Finally, it is noted that the separation variable cannot be overcome by simply varying the distance of the observer to the display. If the observer is too far from the display, the spatial microstructure within the visual pattern is lost, as in the preliminary tests.

References

Guttman, N. and B. Julesz, 1963. Lower limits of auditory periodicity analysis. J. Acoust. Soc. Amer. 35, 610 (L).

Julesz, B., 1962. Visual pattern discrimination. Institute of Radio Engineers Transactions on Information Theory IT–8, 84–92.

Julesz, B. and N. Guttman, 1963. Auditory memory. J. Acoust. Soc. Amer. 35, 1895(A).

Pollack, I., 1969. Depth of sequential auditory information processing. J. Acoust. Soc. Amer. 46, 952–964.

Pollack, I., 1971. Detection of one-, two-, and three-dimensional Markov constraints in visual displays. Acta Psychol. 35, 219–232.

Pollack, I., 1972. Visual discrimination thresholds for one- and two-dimensional Markov spatial constraints. Perception & Psychophysics 12(2A), 161–167.

Rosenblatt, M. and D. Slepian, 1962. *N*th order Markov chains with every *N* variables independent. J. Soc. Industr. Appl. Math. 10, 537–549.

Smith, J.E.K., 1954. Statistical structure and probability learning. Ann Arbor, Mich.: University of Michigan, unpubl. Ph.D. thesis.

Taylor, M. and D. Creelman, 1967. Pest: efficient estimates on probability functions. J. Acoust. Soc. Amer. 41, 782–787.